

# Cracking Activity and Hydrothermal Stability of MCM-41 and Its Comparison with Amorphous Silica-Alumina and a USY Zeolite

A. Corma,<sup>\*,1</sup> M. S. Grande,<sup>\*</sup> V. Gonzalez-Alfaro,<sup>†</sup> and A. V. Orchilles<sup>†</sup>

<sup>\*</sup>*Instituto de Tecnología Química, U.P.V.-C.S.I.C., Avda. de los Naranjos, s/n, 46021 Valencia, Spain; and* <sup>†</sup>*Departament de Ingenieria Química, Universitat de Valencia, Dr. Moliner 50, 46100, Burjasot, Valencia, Spain*

Received May 8, 1995; revised October 4, 1995

It has been found that the cracking activity of MCM-41 for a reaction catalyzed by strong acids site, such as *n*-heptane cracking, is much lower than that of a USY zeolite, and similar to that of amorphous silica-alumina. The higher activity of USY is due to the presence of stronger Brønsted acid sites in the zeolite. In the case of gas oil cracking, the greater accessibility of the large molecules to acid sites in MCM-41 relative to USY makes the difference in activity between these two catalysts much smaller than for the pure hydrocarbon. In the calcined state MCM-41 is more active and gives more gasoline and less gases and coke than amorphous silica-alumina. However, when the catalysts were steamed, the pores of MCM-41 collapsed and its surface area and gas oil cracking was strongly reduced, resulting in a much less active catalyst than the steamed amorphous silica-alumina. An increase in the pore walls diameter from 7 to 11 Å did not solve the hydrothermal stability limitations of the MCM-41. Samples with higher Al content showed a stronger surface area reduction upon steaming. © 1996 Academic Press, Inc.

## INTRODUCTION

Zeolite Y has been, and still is, the heart of FCC catalysts (1–3). The combination of acidity, hydrothermal stability, and pore size has made this zeolite unbeatable as the main active component of cracking catalysts. However, the 7.4-Å pore openings of Zeolite Y prevent the cracking of larger molecules inside the pores. Therefore the cracking of large molecules occurs on the external surface of the crystallites. It is for this reason that the creation of mesopores during hydrothermal treatment and the use of small-crystallite-size Y zeolite show an improvement in gas oil cracking activity (4–7). Even Y zeolites with larger ratios of external to internal surface area exhibit a limited level of bottoms cracking active matrices of silica-alumina are introduced to carry out a precracking of the bulkier molecules present in the higher boiling point fractions (8). However, the amount of active matrix to be used is limited

by the fact that its cracking behavior is much less selective than that of the zeolite. Consequently, more gases and coke are formed on the former and, if operating severity is too high, limitations in the regenerator and gas compressor of the unit result. For the above reasons, much effort is underway to synthesize stable zeolites with pores larger than faujasite. Thus when zeotypes such as VPI-5 (9), cloverite (10), and DAF (11) were discovered, big expectations were opened for their use as FCC catalysts. Unfortunately, their limited hydrothermal stability and/or high production costs have prevented their commercialization.

Very recently a new family of mesoporous aluminosilicates with a regular array of uniform pores of 20–100 Å diameter has been discovered (12, 13). These MCM-41 materials can be synthesized over a large range of framework Si/Al ratios and can develop acidity (14). There is no doubt that the presence of these very large uniform pores combined with acidic properties may open new possibilities for cracking heavier feeds.

In this paper we have studied the potential of a series of MCM-41 materials for cracking vacuum gas oil. Their catalytic activity, selectivity, and hydrothermal stability have been studied and compared to those of a classical amorphous silica-alumina and a USY zeolite. This study allows us to predict the potential use of these materials as catalysts in existing FCC units (FCCU).

## EXPERIMENTAL

### Materials

Three samples of MCM-41 with Si/Al ratios of 14, 100, and 143 (named MCM-41.1, MCM-41.2, MCM-41.3, respectively) were synthesized following the procedure given in Ref. (12), using hexadecyltrimethylammonium (Pan-reac 98 wt%) cation as template, silica (Aerosil Degussa), pseudoboehmite (catapal B, Vista), and sodium aluminate (Carlo Erba) as the aluminum sources. The samples were activated by calcination in N<sub>2</sub> during 1 h at 813 K and

<sup>1</sup> To whom correspondence should be addressed.

TABLE 1

IR Intensity of the Pyridinium Bands and Pyridine Coordinate to Lewis Sites on the Different Catalyst Samples

Desorption temperature (K):	Acidity ( $\mu\text{mol py}$ ) <sup>a</sup>					
	Brønsted			Lewis		
	423	523	623	423	523	623
MCM-41.1	12	6	3	47	34	24
MCM-41.2	1.5	0.6	0.3	3.1	2.3	1.5
MCM-41.3	n.d.	n.d.	n.d.	2.3	1.5	1.5
ASA	12	6	3	37	23	2
USY1		21	9		11	8

<sup>a</sup> From extinction coefficient from (18).

in air during 7 h at the same temperature. They were used in this way as if they were the fresh catalysts introduced in the FCCU. The amorphous silica-alumina sample (25 wt%  $\text{Al}_2\text{O}_3$ ) was provided by Crosfield, named ASA. The USY zeolite (USY1) was prepared by steam calcination of a  $\text{NH}_4\text{NaY}$  sample at 823 K, followed by  $\text{NH}_4^+$  ion exchange and steam calcination at 973 K. The unit cell size and  $\text{Na}_2\text{O}$  content of the final sample was 24.27 Å and 0.03 wt%, respectively. To simulate equilibrium catalysts, the MCM-41 as well as the amorphous silica-alumina and USY zeolite were steamed at 1023 K for 5 h under 100% steam. The unit cell size of USY1.ST was 24.25 Å.

X-ray powder diffraction patterns were carried out, using  $\text{CuK}\alpha$  radiation, on a Phillips PW diffractometer equipped with a graphite monochromator, to characterize the MCM-41 synthesized samples and to determine crystallinity and unit cell size of the USY zeolites.

Surface area measurements were obtained on an ASAP-2000 apparatus following the BET procedure. Pore diameter distribution was obtained using argon as adsorbate and following the BET procedure. Pore diameter distribution was obtained using argon as adsorbate and following the Horvath–Kawazoe method (15).

Solid-state  $^{27}\text{Al}$  and  $^{29}\text{Si}$  MAS NMR spectra were recorded on a Varian Unity VXR-400WB spectrometer at

104.2 and 79.5 MHz respectively, and experimental conditions are included in Ref. (16).

IR spectra were obtained on a Nicolet 710 FTIR spectrophotometer using wafers of  $10 \text{ mg} \cdot \text{cm}^{-2}$  treated in a vacuum cell at 673 K for 16 h. The experiments of adsorptions and stepwise desorption of pyridine have been described before (14). The results given in Table 1 show that the acid strength of USY1 is the highest of the three catalysts, with MCM-41.1 and amorphous silica-alumina having similar acid strengths. This was confirmed by  $\text{NH}_3$  TPD.

### Reaction Procedure

A vacuum gas oil (Table 2) has been cracked in a computer-controlled automated micro-activity test (MAT) unit manufactured by Vinci technologies. This unit can perform in a continuous way up to 8 cycles, i.e., stripping–reaction–regeneration, without personal assistance. The reaction zone and product recovery system have been designed in accordance with ASTM D-3907. The reaction was performed at 773 K, and the catalyst time on stream (TOS) in all experiments was 75 s. Conversion was varied by changing the catalyst to oil ratio in a range of 1.8 to  $6.0 \text{ g} \cdot \text{g}^{-1}$ . This variable was changed by keeping constant the amount of catalyst and changing the amount of oil fed between 0.80 and 2.22 g. Before each experiment the system was purged for 30 min with a  $\text{N}_2$  flow of  $30 \text{ cc} \cdot \text{min}^{-1}$  at the reaction temperature, and then the predesigned amount of gas oil was fed. After this, stripping of the catalyst was carried out for 15 min using  $30 \text{ cc} \cdot \text{min}^{-1}$  of  $\text{N}_2$ . During the reaction and stripping, liquid products were collected in the corresponding glass receivers located at the exit of the reactor which were kept at 275 K by means of a computer-controlled bath. Meanwhile the gaseous products were collected in a gas buret by water displacement. While the gases were automatically analyzed after stripping, in a Varian GC with a two-column system and two detectors (TCD and FID), the catalyst was simultaneously regenerated at 793 K for 3.5 h passing  $30 \text{ cc} \cdot \text{min}^{-1}$  of dry air. The  $\text{CO}_2$  and  $\text{H}_2\text{O}$  generated during coke combustion were also automatically analyzed by continuous sampling using a Varian GC

TABLE 2

Properties of the Vacuum Gas Oil Feed

Density 60°C (g/cc)	0.859									
15°C (g/cc)	0.888									
Aniline Point (%wt)	76.5									
Sulphur (%wt)	1.7									
$\text{N}_2$ (ppm)	125									
Average molecular weight	383									
Refraction index at 60°C	1.48254									
KUOP	11.9									
Distillation curve D-1160 (°C)										
IBP	10	20	30	40	50	60	70	80	90	FBP
212.6	321.6	351.8	370.8	384.6	399.7	406.9	415.1	427.2	443.1	463.5

TABLE 3  
Chemical Composition of the Catalysts

	Si/Al	Al <sub>2</sub> O <sub>3</sub> (%)	Na <sub>2</sub> O (%)
MCM-41.1	14 <sup>a</sup>	6.4	0.2
MCM-41.2	100 <sup>a</sup>	0.8	—
MCM-41.3	143 <sup>a</sup>	0.7	—
USY1	100	1.79	0.03
ASA	2.5	25	—

<sup>a</sup> Gel Si/Al ratio.

chromatograph. Data of CO<sub>2</sub> and H<sub>2</sub>O were time accumulated and in this way the total coke and its C/H ratio were determined. Liquid analysis was performed by simulated distillation (ASTM-D 2887). *n*-Heptane cracking experiments were carried out in a fixed-bed, glass tubular reactor, at atmospheric pressure, and at reaction temperature of 723 K. Two grams of *n*-heptane was fed at different TOS, and the amount of catalyst was changed to modify the catalyst to oil ratio in the 0.05–0.43 g · g<sup>-1</sup> range. The general experimental procedure was described previously (17). Liquid and gaseous products were analyzed by GC in a HP-5890 II GC equipped with TCD and FID detectors. Following this procedure, curves of conversion versus 1/WHSV and yields versus total conversion were generated, for comparison of the activity and selectivity of different catalysts.

## RESULTS AND DISCUSSION

### Behavior of Calcined MCM-41

In Table 3 the chemical composition of the MCM-41 samples used in this study are given.

The mesoporous MCM-41 aluminosilicate samples produced were characterized by a broadband at low angles in the XRD spectrum, a narrow distribution of pore sizes, and surface areas above 800 m<sup>2</sup> · g<sup>-1</sup> (Table 4). From the XRD spectra (Fig. 1), samples MCM-41.2 and MCM-41.3 show a well-defined hexagonal pattern, whereas the pore packing is less ordered in MCM-41.1. No improvement in pore

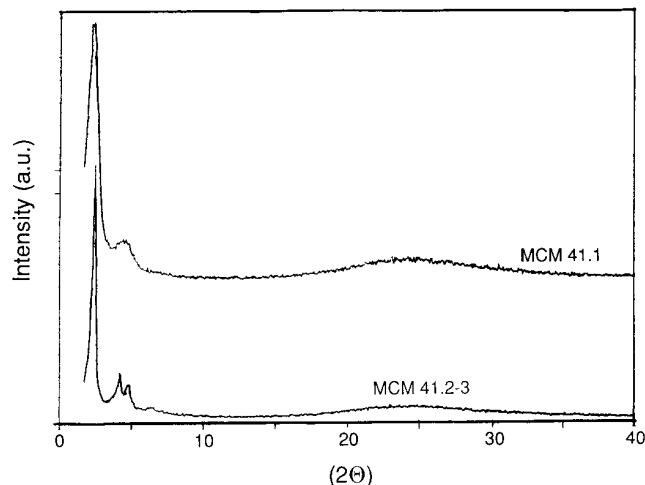


FIG. 1. XRD spectra of MCM-41 samples.

ordering is observed when changing the OH/SiO<sub>2</sub> ratio in the MCM-41.1 synthesis, indicating that, under the synthesis conditions used here, it is difficult to incorporate high amounts of Al if alkaline ions are not present during the synthesis. The values of surface area and pore diameter are consistent with the above observation (Table 4).

Previous MAS <sup>27</sup>Al NMR results on as-synthesized MCM-41 have shown all of the Al to exist in tetrahedral coordination (Al<sup>IV</sup>; 50–52 ppm), with intensities in reasonable agreement with its Si/Al ratio obtained by chemical analysis (16). It was also observed that after calcination the intensity of the Al<sup>IV</sup> peak strongly decreased as Al<sup>VI</sup> octahedral species formed, indicating that the samples were partially dealuminated.

TABLE 4

### Surface Area and Pore Diameter of the Catalyst Samples

	BET area (m <sup>2</sup> /g)	Pore volume (cm <sup>3</sup> /g)	Average diameter of pores (Å) <sup>a</sup>
MCM-41.1	837	0.781	20
MCM-41.2	1031	0.527	20
MCM-41.3	877	0.600	33
USY1	551	0.349	
ASA	268	0.282	

<sup>a</sup> Argon measured.

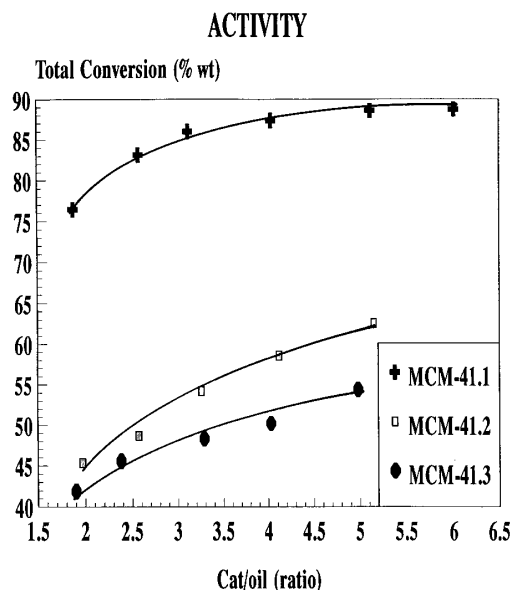


FIG. 2. Activity for cracking of gas oil for calcined MCM-41 samples.

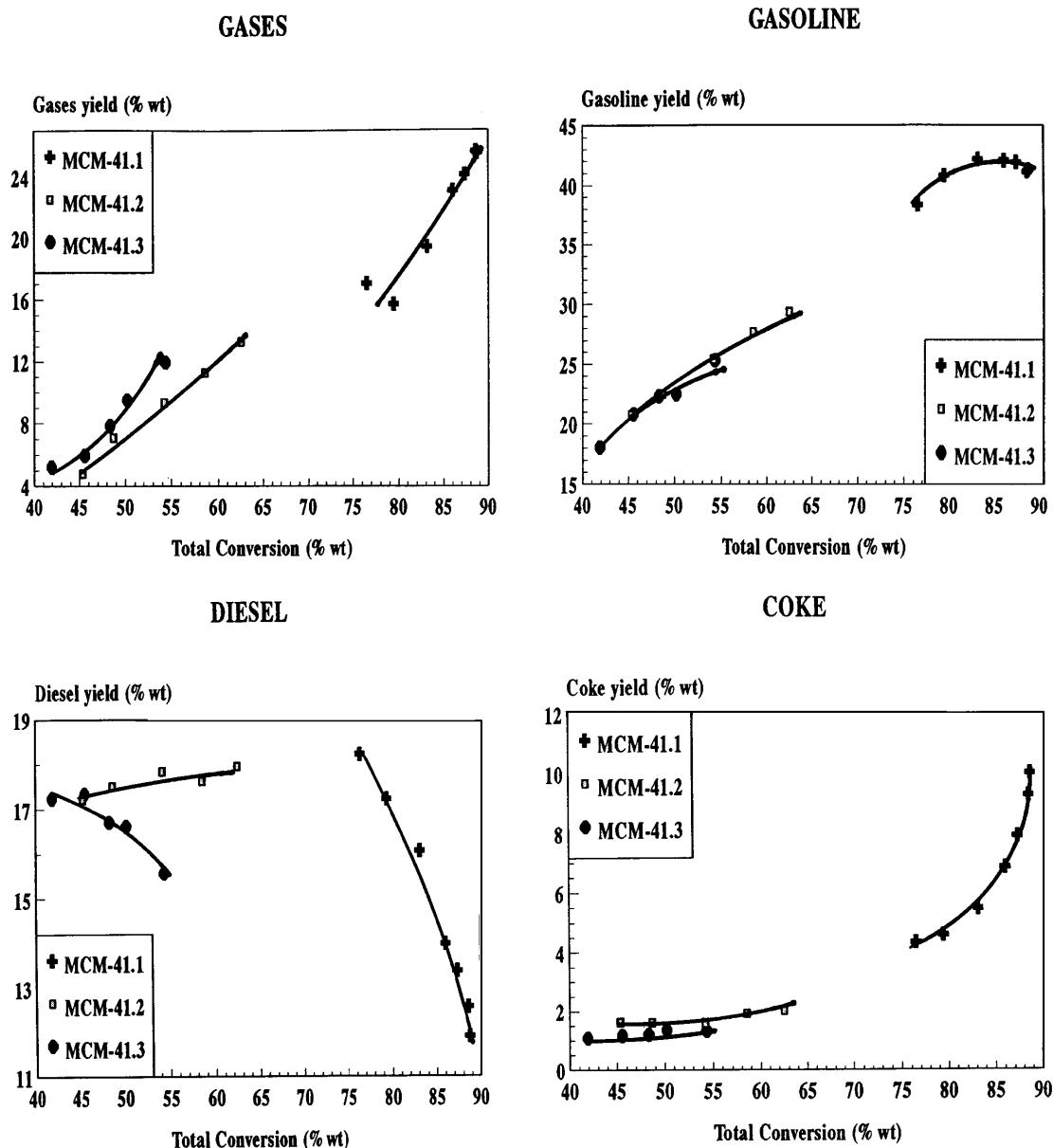


FIG. 3. Selectivity to different products vs total conversion for cracking of gas oil for calcined MCM-41 samples.

In any case, the relative intensity of the  $\text{Al}^{\text{IV}}$  peak of the calcined samples indicates that MCM-41.1 has a more tetrahedral Al, and consequently more Brønsted acidity, than the other MCM-41 samples. This is confirmed by the intensity of the pyridinium band ( $1545\text{ cm}^{-1}$ ), remaining after desorption of pyridine at 423 K (Table 1). Moreover the intensity of the pyridine band associated with Lewis acid sites ( $1455\text{ cm}^{-1}$ ) increases when decreasing the Si/Al ratio of the synthesized zeolite. This indicates that higher Al content in the original samples results in more extraframework Al and, consequently, a larger amount of Lewis acid sites.

In the case of fresh catalysts (calcined MCM-41 sam-

ples), the gas oil cracking results (Fig. 2) are in good agreement with the Brønsted acidity remaining after calcination (Table 1); i.e., the lower initial framework Si/Al ratio of the MCM-41.1 sample yields higher gas oil cracking activity. Moreover the curves giving yields versus total conversion (Fig. 3) show that the three MCM-41 catalyst fall close to unique selectivity curves. This indicates that the nature of the active sites is similar for the MCM-41 samples with different framework Si/Al ratios. The conclusion appears quite reasonable if one takes into account that at the relatively high "framework" Si/Al ratios of the calcined catalysts, the acidic sites should be isolated and therefore very similar in their acid characteristics.

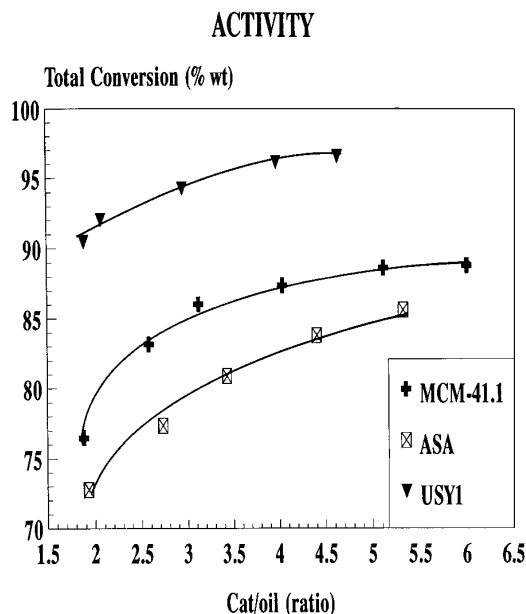


FIG. 4. Activity for cracking of gas oil for MCM-41.1, ASA, and USY1.

#### Comparison of the Behavior of MCM-41, Amorphous Silica-Alumina, and USY Zeolite

When the gas oil cracking conversion on these three catalysts is compared (Fig. 4) it can be seen that the order of activity is  $USY1 > MCM-41.1 > ASA$ . On a qualitative basis the order of activity is the same as the amount of Brønsted acid sites present in each catalyst except for the ASA, which presents the same Brønsted acidity as MCM-41. The same order was found when the activity was quantified by the first-order kinetic rate constant ( $K$ ) and by the  $K$  normalized for the Al content of the samples (Table 5). These results already put forward the possible benefit derived from the regular pore distribution in the case of MCM-41.

To differentiate between the catalytic effects due to intrinsic site activity and reactant site accessibility, the cracking of *n*-heptane was also carried out on these catalysts. Indeed, *n*-heptane can easily diffuse in the pores of all three catalysts and therefore should indicate the intrinsic acid cracking activity of USY1, MCM-41.1, and ASA cat-

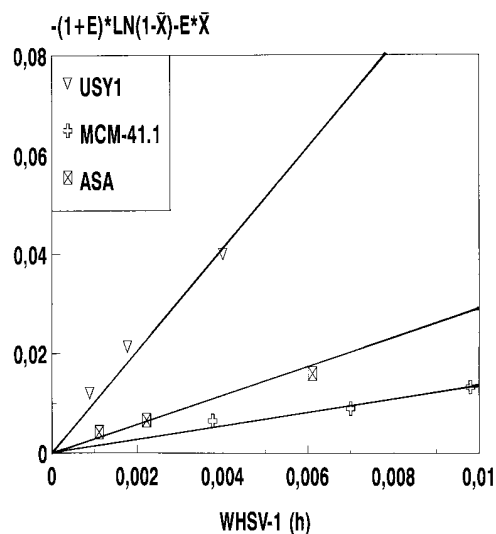


FIG. 5. Pseudo-first-order rate constant for cracking for *n*-heptane by MCM-41.1, ASA, and USY1.

alysts. From the results presented in Fig. 5, the calculated kinetic rate constants for *n*-heptane cracking, together with *n*-heptane cracking activity per Al site, are given in Table 6. The data in Tables 5 and 6 indicate that the intrinsic activity for *n*-heptane cracking is 139 times larger on USY1 than on MCM-41.1, while in the case of gas oil that ratio is much lower (11). These interesting results show that the larger pores present in MCM-41.1 facilitate the cracking of large molecules present in the gas oil feed, whose diffusion in the smaller pores of the USY zeolite is much more restricted.

When gas oil cracking selectivity results are compared Fig. 6, the behavior of MCM-41 is more similar to that of USY, producing more gasoline, and less gases and coke, than amorphous silica-alumina. These results could be explained by considering that the amount of nontetrahedral alumina, which is known to catalyze a less selective cracking (3), is larger on the 25 wt%  $Al_2O_3$  containing silica-alumina and would be responsible for the higher selectivity to gases and coke of the amorphous material. In addition, the probably larger tortuosity factor of the pores in the ASA will also favor consecutive reactions leading to gases and coke. Note that the selectivity to dry gases, that are clear secondary products, will support that explanation.

TABLE 5

#### First-Order Kinetic Rate Constant for Gas Oil Cracking

Sample	First-order kinetic rate $K^a$	$K/Al/(Al + Si)$
MCM-41.1	2.04	29.14
ASA	1.71	19.00
USY1	3.22	322

<sup>a</sup> Calculated from a first-order rate expression  $\ln(1 - x)$  at cat/oil ratio 4.

TABLE 6

#### First-Order Kinetic Rate Constants for *n*-Heptane Cracking

Sample	First-order kinetic rate ( $h^{-1}$ ) <sup>a</sup>	$K/Al/(Al + Si)$
MCM-41.1	0.6211	8.873
ASA	3.20	35.56
USY1	12.37	1237

<sup>a</sup> Calculated from plot stop of  $-\ln(1 - x)$  v.s.  $WHSV^{-1}$ .

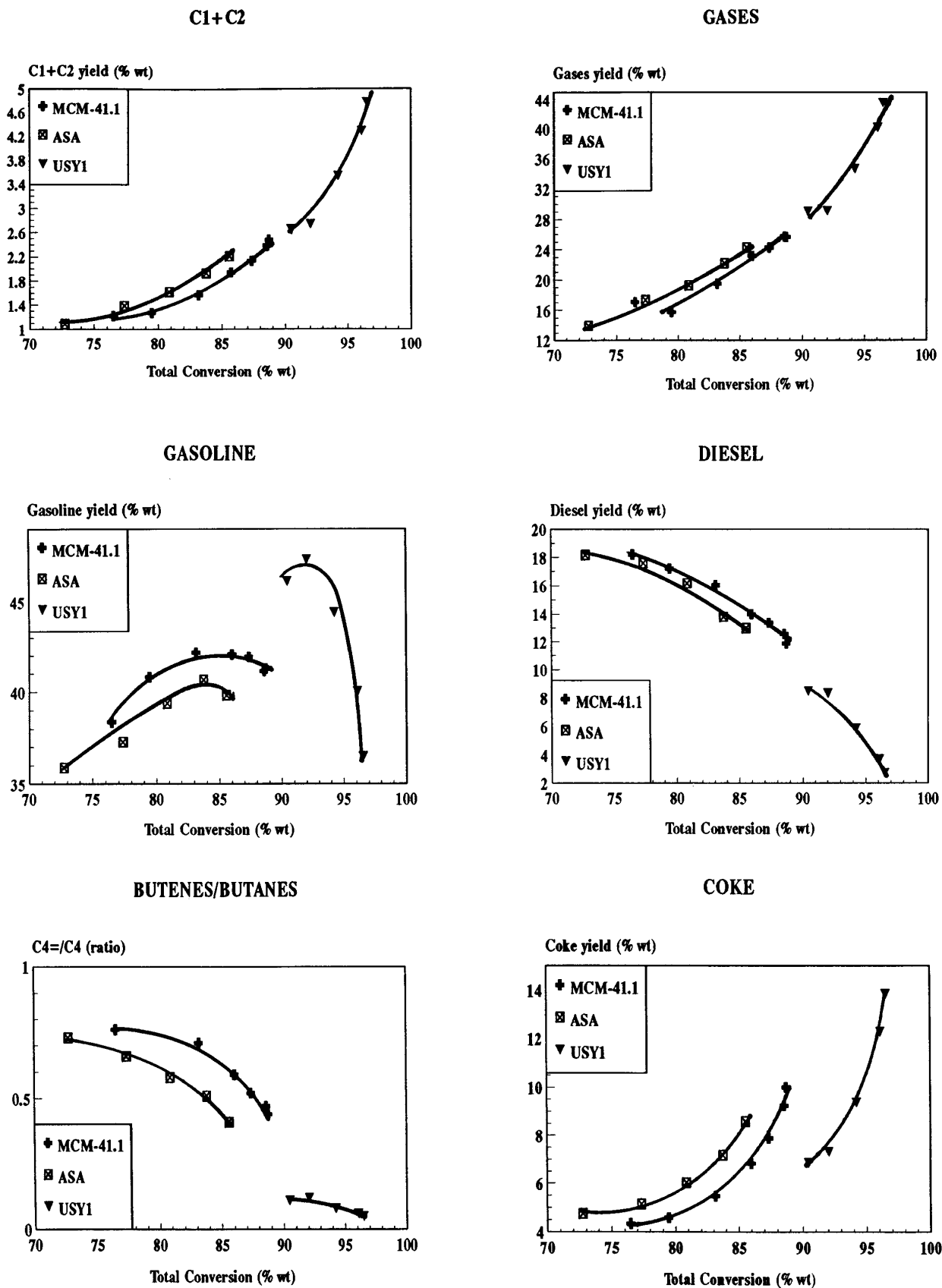


FIG. 6. Selectivity to different products vs total conversion for cracking of gas oil for MCM-41.1, ASA, and USY1.

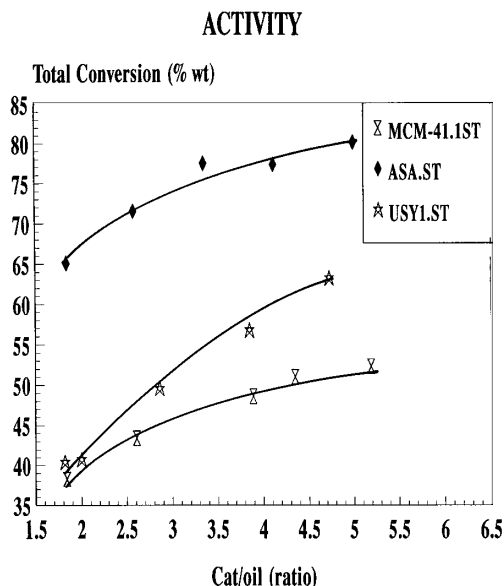


FIG. 7. Activity for cracking of gas oil for steamed MCM-41.1, ASA, and USY1.

If the gas oil cracking results obtained on the calcined MCM-41.1 sample look attractive, one should take into account that in the regenerator of the FCCU, the catalyst is subjected to temperatures on the order of 1023 K in the presence of steam. Therefore, more realistic conclusions on the practical possibilities of the FCC catalyst obtained by testing the catalytic activity of a potential cracking catalyst after it has been deactivated by a steam calcination. We have done that by steaming the catalysts at 1023 K for 5 h in the presence of 100% steam.

When the gas oil cracking activity of the steamed samples was measured, it was found that MCM-41 is much less active than either USY or amorphous silica-alumina (Fig. 7).

The results (Table 7) show that steamed samples have suffered a strong reduction in surface area, and XRD show that only the USY zeolite has preserved its structure. On the other hand the pores of the MCM-41 samples have mostly collapsed, and their surface area is now lower than that of the steamed amorphous silica-alumina. It should be noted that a larger surface area retention occurred on MCM-41.3 sample, which has a much lower Al content.

TABLE 7

Surface Area of the Steamed Samples

	BET(m <sup>2</sup> /g)
MCM-41.1ST	81
MCM-41.2ST	84
MCM-41.3ST	347
ASA.ST	116
USY1.ST	213

Thus, we have to conclude that even though the pore structure and acid characteristics of the calcined MCM-41 sample studied here is active and selective to carry out the cracking of gas oil, its hydrothermal stability is not good enough to resist the very drastic conditions present in the regenerator. In this case cracking activity would be lost due to a "dealumination" process, as well as by the collapse of the pores, especially in samples containing larger amounts of Al. Thus, unless the hydrothermal stability could be strongly improved, these type of materials will not be adequate to be used in actual FCC catalysts.

We have tried to improve the hydrothermal stability of the MCM-41 structure by increasing the size of the walls. To do that a sample was prepared following the procedure described in (18). The MCM-41 sample prepared contained 5.9% Al<sub>2</sub>O<sub>3</sub>, has a BET surface area of 792 m<sup>2</sup>·g<sup>-1</sup>, a pore diameter of 38 Å, and a pore wall diameter of 11 Å instead of the 7 Å of MCM-41.1. After steam treatment at 1023 K for 5 h, the pores collapsed and the surface area was reduced to 89 m<sup>2</sup>·g<sup>-1</sup>, indicating that even with pore walls containing three to four tetrahedra, the structure is not stable enough to resist the conditions in an FCC regenerator.

## CONCLUSION

It has been found that calcined MCM-41 samples are active and selective catalysts for cracking vacuum gas oil. The activity and selectivity of samples synthesized with lower Si/Al ratio (<100) are better than those of amorphous silica-alumina cracking catalysts (25 wt% Al<sub>2</sub>O<sub>3</sub>). It appears that in the mesoporous materials the larger pore sizes have a beneficial effect on cracking the large size molecules present in gas oil. The acid strength of the sites in MCM-41 and its catalytic activity for cracking a small molecule such as *n*-heptane is lower than that of USY. However, the site accessibility due to its mesoporous structure can partially compensate, in the case of gas oil cracking, for the lower intrinsic cracking activity of MCM-41.

When catalysts were steamed to simulate an equilibrium FCC catalyst, the pores of MCM-41 collapsed and its surface area and gas oil cracking activity strongly diminish, resulting in a much less active catalyst than the steamed amorphous silica-alumina. This was so, even with a sample prepared with pore wall thickness of 11 Å.

## ACKNOWLEDGMENT

Financial support by the Dirección General de Investigación Científica y Técnica of Spain (Project MAT 94-0359-C02-02) is gratefully acknowledged.

## REFERENCES

1. Scherzer, J., "Octane Enhancing Zeolitic FCC Catalysts." Dekker, New York, 1990.
2. Biswas, J., and Maxwell, I. E., *Appl. Catal.* **63**, 197 (1990).

3. Corma, A., *Stud. Surf. Sci. Catal.* **49**, 49 (1989).
4. Patzelova, V., and Jaeger, N. I., *Zeolites* **7**, 240 (1987).
5. Lynch, J., Raatz, F., and Dufresne, P., *Zeolites* **7**, 333 (1987).
6. Rajagopalan, K., Peters, A. W., and Edwards, G. C., *Appl. Catal.* **23**, 69 (1986).
7. Camblor, M. A., Corma, A., Martínez, A., Mocholí, F. A., and Pérez-Pariente, J., *Appl. Catal.* **55**, 65 (1989).
8. O'Connor, P., Gerritsen, L. A., Pearce, J. R., Desai, P. H., Yanik, S., and Humpries, A., *Hydrocarbon Process. Int.*, Ed. **70**, 76 (1981).
9. Davis, M. E., Montes, C., Hathaway, P. E., and Garcés, J. M., *Stud. Surf. Sci. Catal.* **49**, 199 (1989).
10. Estermann, M., McCusker, L. B., Baerlocher, C., Merrouche, A., and Kessler, H., *Nature* **352**, 320 (1991).
11. Huo, Q., Xu, R., Li, S., Ma, Z., Thomas, J., Jones, R. H., and Chippendale, A. M., *J. Chem. Soc. Chem. Commun.*, 875 (1992).
12. Beck, J. S., Chu, C. T. W., Johnson, I. D., Kresge, C. T., Leonowicz, M. E., Roth, W. J., and Vartuli, J. C., WO 91/11390 (1991).
13. Beck, J. S., Calabro, D. C., McCullen, S. B., Pelrine, B. P., Schmitt, K. D., and Vartuli, J. C., U.S. Patent 5145816 (1992).
14. Corma, A., Fornés, V., Navarro, M. T., and Pérez-Pariente, J., *J. Catal.* **148**, 569 (1994).
15. Horvath, G., and Kawazoe, K., *J. Chem. Eng. Jpn.* **16**, 470 (1983).
16. Kolodziejski, W., Corma, A., Navarro, M. T., and Pérez-Pariente, J., *Solid State Nucl. Magn. Reson.* **2**, 253 (1993).
17. Corma, A., Monton, J. B., and Orchillés, A. V., *Appl. Catal.* **23**, 255 (1986).
18. Constel, N., Di Renzo, F., and Fajula, F., *J. Chem. Soc. Chem. Commun.*, 967 (1994).